Supplemental Information

Effect of Hydrophilic Defects on Water Transport in MFI Zeolites

Thomas Humplik[a], Rishi Raj[a,+], Shalabh C. Maroo[b], Tahar Laoui[c], and Evelyn N. Wang[a,*]

[a]Department of Mechanical Engineering, Massachusetts Institute of Technology, Cambridge MA 02139
[b]Department of Mechanical & Aerospace Engineering, Syracuse University, Syracuse NY 13244
[c]Department of Mechanical Engineering, King Fahd University of Petroleum and Minerals, Dhahran, Saudi Arabia

[+]Currently with: Department of Mechanical Engineering, Indian Institute of Technology Patna, Bihar, India
[*]Corresponding Author: Tel: +1 617 324 3311, email: enwang@mit.edu (E. N. Wang)

S.1 Supplemental data

Table S1. Volume, surface area, and area ratio of MFI zeolites synthesized in this study. Note that the surface area ratio for all samples is greater than 1000, thereby limiting the experimental analysis to the internal pore volume.

Zeolite	Surface Area $(\mu m)^2$	Volume $(\mu m)^3$	Int/Ext Area Ratio
INF	33.25	8.25	1618
1000	22.25	5.25	1539
300	18	4.5	1631
200	17.2	4.2	1593
100	10	2	1305

S.2 Comparison with Cailliez[1] silanol defect models

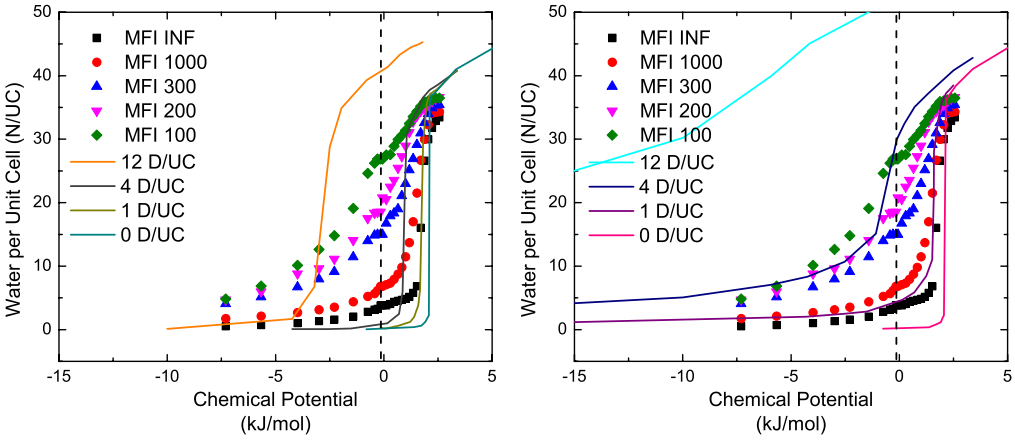

Figure S1. Magnified view of the comparison of the experimental data with Cailliez's weak defect model (A) and strong defect model (B). Note that the vapor to liquid phase transformation occurs at a chemical potential of -0.1 kJ/mol.

Figure S1 shows the zoomed in views of the comparison between the Cailliez weak (S1A) and strong (S1B) defect model and our experiments. Note that the vapor to liquid phase change occurs at a chemical potential of $\approx$ -0.1 kJ/mol. For the weak defect model, the infiltration into the porous network occurs almost completely at a single value for the chemical potential and subsequently the pressure. This behavior is characteristic of capillary condensation, although the definition is extended here since it occurs above the saturation pressure[2,3]. The experimental results do not agree with this model. However, the stronger defect model exhibits water infiltration both at pressures below and above the saturation pressure, which is the trend that is observed with experiments. As a side note, both Cailliez models tend to overestimate the amount of water that infiltrates into the pores, which indicates that further refinements to the models are required to accurately depict the experimental behavior.

S.3 Sorption analysis and transport properties

Figure S2 shows the time-dependent uptake behavior for water that adsorbed into the zeolites at a relative pressure of 0.4. The diffusivity, which was estimated from the slopes of the curves, decreased with an increasing defect density. At each step (we used steps of $P/P_o = 0.1$) in the relative pressure (both during adsorption and desorption), the transient increase in mass was plotted as a function of the square root time. The diffusivity was estimated using the short time ($0.2 < M_t/M_\infty < 0.6$) analytical solution to Fick's law:

$$\frac{M_t}{M_\infty} \approx \frac{2A}{V}\left(\frac{D_t t}{\pi}\right)^{1/2}$$

The results for the deduced diffusivity over the full vapor pressure range are shown in Figure S3A. The error bars signify the standard deviation in the measurements. The estimated diffusivity values are fairly constant over the range of pressures tested. Furthermore, the measured diffusivity between adsorption and desorption did not vary significantly, indicating that the mass transfer resistance into and out of the zeolites was the limiting resistance in the measurements (*i.e.,* the bulk vapor diffusion in the testing cell was considered to be negligible).

The solubility was also quantified so that the permeability could ultimately be determined. The highest solubility was typically measured at the lowest relative pressure (0.05), since the largest quantity of water was adsorbed in this range. This behavior is usual for zeolites, as an anhydrous zeolite (primarily due to the hydrophilic defects) has the highest affinity for water adsorption (this initial adsorption also corresponds to the maximum heat of adsorption during water uptake, although this quantity was not

measured in these experiments)[4]. The solubility plateaus as the relative pressure increases which is a characteristic of adsorption isotherms which follow Henry's Law[5].

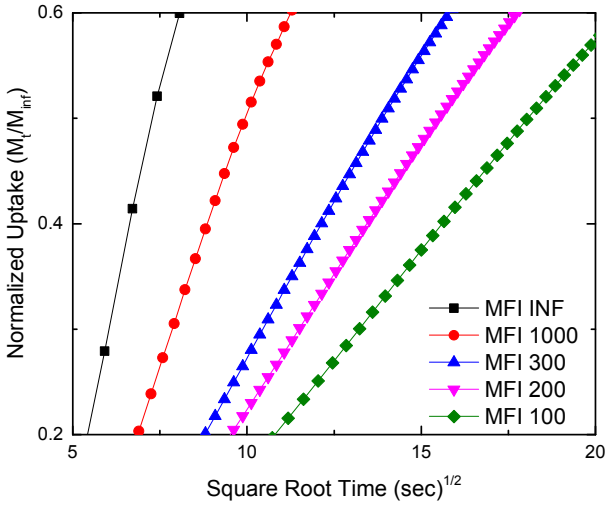

Figure S2. Example adsorption curve for various Si/Al ratio MFI zeolites taken at a relative pressure of 0.4. The approximate linear response indicates a Fickian diffusion process.

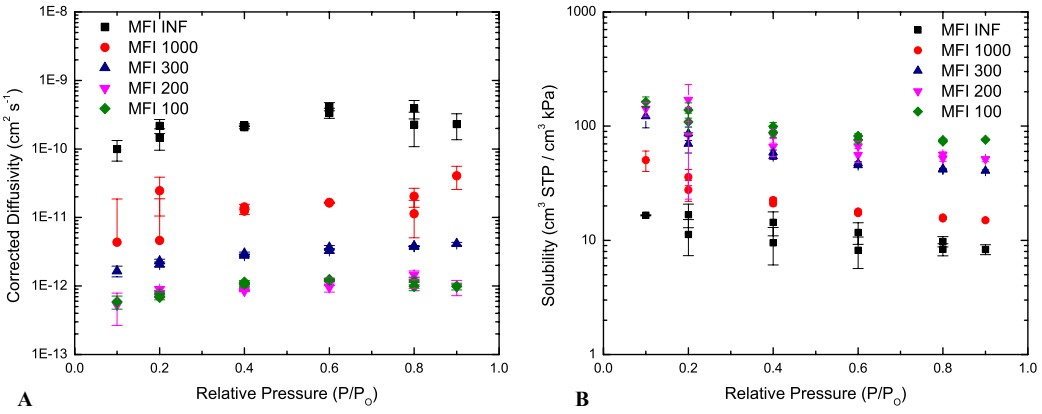

Figure S3. The complete data set of both the diffusivity (A) and solubility (B) as a function of the relative pressure.

Finally, the permeability was determined by taking the product of the diffusivity and solubility. As with the previous measurements, the permeability did not change as a function of the external pressure, indicating that the transport is constant for the range of

pressures investigated. The least defective zeolite, Silicalite-1 (MFI INF), was estimated to have the largest water permeability of the zeolites investigated in this study.

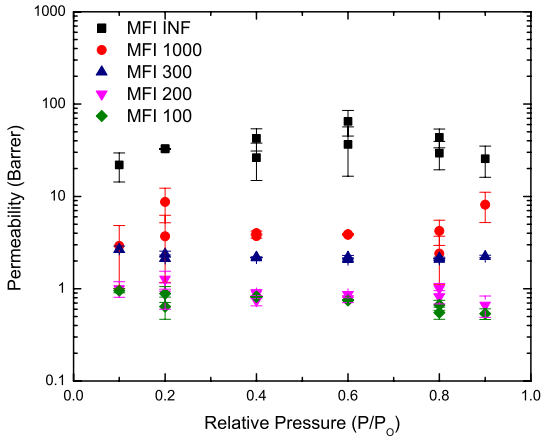

Figure S4. The complete data set of the permeability as a function of the relative pressure. The permeability decreased as the defect density increased. Note that 1 Barrer is 3.06×10^{-16} (mol m)$(m^2\ s\ Pa)^{-1}$ at STP.

S.4 Defect density calculations

Following the procedure of Olson *et al.,* the defect density was approximated by extrapolating a linear fit in the low relative pressure range in Figure S5, and obtaining the intercept of the abscissa (which correlated to a number of water molecules per unit cell). The defect density was calculated by assuming that each defect adsorbs ≈ 4 water molecules at zero relative pressure (*i.e.*, the defect density is ¼ of the number of adsorbed molecules at 'zero' pressure)[6]. The quantified defect density is shown in Table 1.

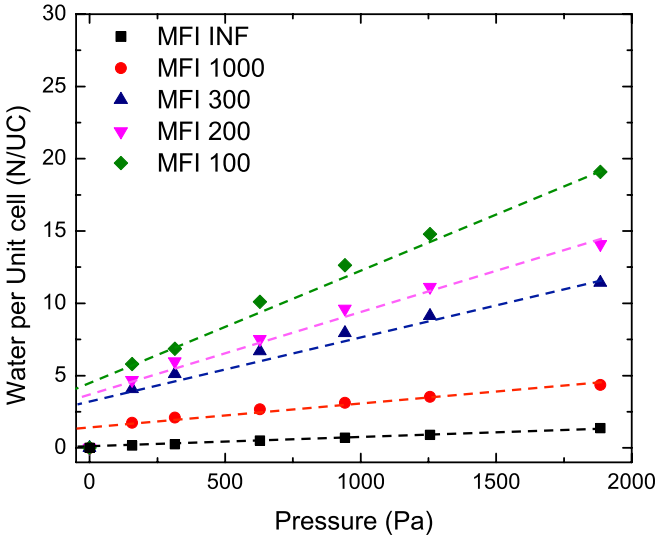

Figure S5. A magnified view of the low relative pressure adsorption isotherms for the various zeolites studied. The dashed line corresponds to a linear fit which, when extrapolated to the intercept of the abscissa, provides an estimate of the defect density.

S.5 Micropore Volume using Nitrogen Sorption

The nitrogen adsorption isotherms of these MFI zeolites are provided to show that the framework pore volume for all zeolites is approximately equivalent (*i.e.,* the introduction of aluminum does not collapse the pore structure). The micropore volume of the zeolites was probed by carrying out physisorption of nitrogen at 77 K (ASAP 2020, Micromeretics). The samples were dried and degassed for 5 hours at 350 °C and at a pressure of 10 μm Hg prior to the tests. The adsorption isotherms are shown in Figure S6 and the t-plot micropore volume is shown in Table S2. The t-plot micropore volume was estimated by a linear regression fit in the partial pressure range of 0.5 – 0.7 to determine the y-intercept of each zeolite (the intercept corresponds to the framework micropore volume).

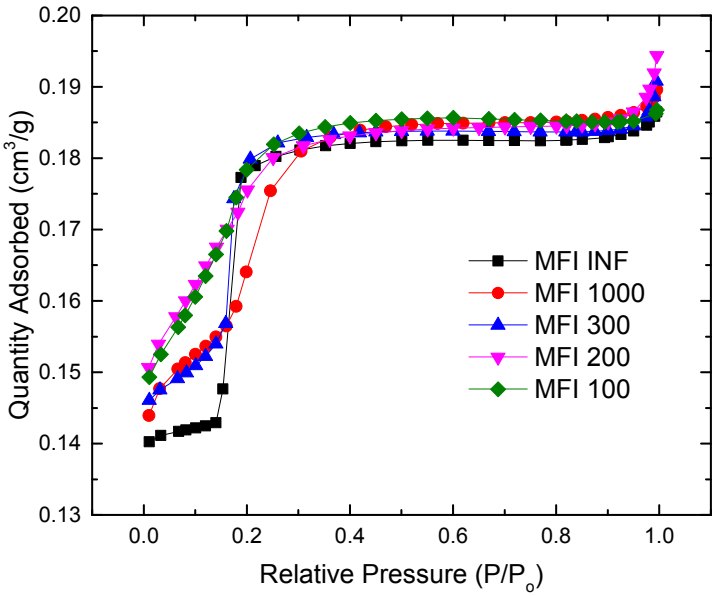

Figure S6. Nitrogen sorption isotherms for MFI zeolites with a varying Si/Al ratio. The calculated micropore volumes are shown in Table S2. There was no observable change in the micropore volume between the zeolites, which indicates that the internal pore structure is unaffected by the inclusion of the defects.

Table S2. Calculated micropore volume of MFI zeolites made using the t-plot method.

Zeolite	Micropore Volume (cm^3/g)
MFI INF	0.180
MFI 1000	0.183
MFI 300	0.183
MFI 200	0.182
MFI 100	0.184

S.6 Boundary Conditions for Diffusion Measurements.

For each step change in the relative pressure, an additional amount of water would adsorb or desorb (depending on the direction of the step change). In the information below, we show an example of the boundary conditions for a step change during adsorption run. The initial pressure condition was $P/P_o = P_1$, and the step in the relative

pressure increased the test cell relative pressure to $P/P_o = P_2$. The quantity q ($V_{ads,\ water}/V_{zeolite,}$) corresponded to the adsorption quantity in cm^3 (STP)/cm^3 zeolite.

$$t < 0,\ P_{Rel} = P_1,\ q = q_{P1}$$
$$t = 0,\ P_{Rel} = P_2,\ q = q_{P1}$$
$$t \rightarrow \infty,\ P_{Rel} = P_2,\ q = q_{P2}$$
$$m_t/m_\infty = q(t)/q_{P2}$$

References

(1) Cailliez, F.; Stirnemann, G.; Boutin, A.; Demachy, I.; Fuchs, A. H. Does Water Condense in Hydrophobic Cavities? a Molecular Simulation Study of Hydration in Heterogeneous Nanopores. *J. Phys. Chem. C.* **2008**, *112*, 10435–10445.

(2) Eroshenko, V.; Regis, R.; Soulard, M.; Patarin, J. Energetics: a New Field of Applications for Hydrophobic Zeolites. *J. Am. Chem. Soc* **2001**, *123*, 8129–8130.

(3) Rouquerol, J.; Rouquerol, F.; Sing, K. S. W. Absorption by Powders and Porous Solids; Academic Press, 1998.

(4) Nagao, M.; Morimoto, T. Differential Heat of Adsorption and Entropy of Water Adsorbed on Zinc Oxide Surface. *J. Phys. Chem.***1969**, *73*, 3809–3814.

(5) Hill, S.; Seddon, D. The Hygroscopic Nature of H-ZSM--5. *Zeolites* **1985**, *5*, 173–178.

(6) Olson, D. Kokotailo, G. Lawton, S. Meier. Crystal structure and structure related properties of ZSM-5. *J. Phys. Chem.* **85**, 2238–2243 (1981).